Dissociative adsorption of O_2 molecules on O-precovered Fe(110) and Fe(100): Density-functional calculations

Piotr Błoński,[1,*] Adam Kiejna,[2,†] and Jürgen Hafner[1,‡]
[1]*Fakultät für Physik and Center for Computational Materials Science, Universität Wien, Sensengasse 8/12, A-1090 Wien, Austria*
[2]*Institute of Experimental Physics, University of Wrocław, Plac M. Borna 9, PL-50-204 Wrocław, Poland*
(Received 31 January 2008; published 17 April 2008)

The dissociative adsorption of O_2 molecules on clean and oxygen-precovered Fe(110) and Fe(100) surfaces has been studied from first principles. For the relatively open Fe(100) surface, we find that along the most favorable reaction channel, O_2 dissociation remains a nonactivated process up to almost full monolayer coverage. The differential heat of adsorption decreases only slowly with increasing oxygen precoverage. The potential energy profile for dissociation shows a dip, which is indicative of the formation of a very short-lived nonmagnetic peroxo precursor. On the close packed Fe(110) surface, the differential heat of adsorption begins to decrease already at a modest precoverage. For dissociation on a surface precovered with about 0.44 monolayer of oxygen, a low barrier begins to appear in the entrance channel. In the transition state, the incoming molecule is in a superoxo state with a magnetic moment of $1\mu_B$. Our results are discussed in relation to the electronic and magnetic properties of the partially precovered surfaces and to the available experimental results.

DOI: 10.1103/PhysRevB.77.155424 PACS number(s): 68.43.Bc, 68.43.Fg, 73.20.Hb, 71.15.Mb

I. INTRODUCTION

The adsorption of oxygen molecules on a metal surface is a very common process that is of fundamental importance in oxidation, catalysis, and corrosion. The adsorption of small diatomic molecules such as oxygen may be molecular or dissociative, while dissociation may be activated or nonactivated, may be a direct process, or may occur via a molecular precursor state. Because of the importance of the Pt-group metals as oxidation catalysts, considerable effort has been spent in investigating oxygen dissociation on these surfaces. Detailed density-functional simulations of the adsorption process on the (111) surfaces of these metals[1,2] demonstrated that molecular oxygen dissociates via a molecular precursor state. Two distinct molecular precursors: a paramagnetic superoxo-like (O_2^-) and peroxo-like (O_2^{2-}) nonmagnetic states have been identified. On Pt(111), the precursor is relatively stable, with a barrier for dissociation that is nearly of equal height as the desorption energy. This facilitates the experimental investigation of the precursors, which has confirmed the theoretical predictions.[3] Similar precursor states have also been predicted to exist on Pd(111) and Ni(111) surfaces, but on these metals, dissociation is facilitated by a lower reaction barrier.[2] On noble metal surfaces, O_2 dissociation is an activated process, but very recently Alatalo *et al.*[4] showed that on Cu(100) surfaces, a "steering" effect (similar to the one discussed first for H_2 dissociation[5,6] on Rh, Pd, and Ag surfaces) may help to find a low-barrier dissociation channel for low kinetic energies. On more reactive clean surfaces such as those of Fe, dissociation on the clean surfaces is known to be a direct nonactivated process. However, less is known on the dissociation process on surfaces that are at least partially precovered with adsorbed oxygen atoms.

Experimental investigations[7–17] as well as our previous theoretical work on the adsorption of atomic oxygen on the (110) and (100) surfaces of Fe (Refs. 18 and 19) revealed interesting differences in the reactivities of these surfaces. At high temperature, oxygen adsorption on the (100) surface leads to the formation of a $p(1\times1)$ monolayer (ML), which was identified as a two-dimensional FeO(100) oxide film with a local magnetic moment on the Fe atoms comparable to the local moment in bulk antiferromagnetic Fe oxides and larger than the moment on the surface atoms on a clean Fe(100) surface. The formation of a compact overlayer is preceded by the formation of $p(2\times2)$ and $c(2\times2)$ superstructures at lower oxygen coverages. At low temperatures, up to a coverage of $\Theta\sim0.8$ ML, the sticking probability S of impinging oxygen molecules remains close to unity, followed by a very sharp decrease to almost zero sticking. These studies indicate that at low temperature, adsorption of O_2 on Fe(100) occurs through a mobile precursor followed by disordered dissociative adsorption. Initially, O atoms occupy fourfold hollow sites, but at higher coverages, occupation of bridge sites has also been reported. At room temperature, a different behavior was observed: S remains approximately constant up to $\Theta\approx0.35$ ML, followed by a linear decrease up to $\Theta\approx1$ ML.[7–10]

On the close packed Fe(110) surface, at high temperatures saturation occurs already at $\Theta\approx0.4$ ML, preceded by the formation of $c(2\times2)$ and $c(3\times1)$ superstructures. The sticking probability decreases linearly up to saturation, followed by a minimum and, subsequently, a maximum at higher oxygen exposure. The minimum in S marks the onset of the formation of an oxide film. The surface of the Fe oxide formed on Fe(110) is ferromagnetically ordered with an alignment of the magnetization antiparallel to that of the substrate.[20–23] Originally, this has been interpreted in terms of an antiparallel coupling of the moments in an FeO(111) surface and the underlying Fe(110) substrate but, alternatively, the formation of an $Fe_3O_4(111)$ instead of an FeO(111) layer has been proposed.[21] The mismatch between the FeO(111) and Fe(110) interfaces prevents the growth of a thicker FeO layer and induces the growth of a ferrimagnetic Fe_3O_4 film on top of the FeO layer.[11–17]

Very recently, the growth, structure, and morphology of ultrathin FeO(111) films on a Fe(110) surface, which were formed by exposure to atomic or molecular oxygen, were investigated by Busch *et al.*[24] by using various experimental techniques. This investigation demonstrated that for an oxidation by atomic instead of molecular oxygen, the gas exposure required for growing an FeO film can be reduced by almost 2 orders of magnitude because dissociation and sticking do not limit the growth process. Also, only the exposure to atomic oxygen leads to the formation of a well ordered FeO(111) film with a low defect concentration. However, ion-beam triangulation experiments show that the formation of a well ordered FeO(111) film is hampered by the mismatch between the rectangular geometry of the Fe(110) surface and the hexagonal geometry of the FeO(111) planes. These observations agree with our result[19] that on Fe(110), the adsorption of atomic oxygen remains an unactivated process up to full monolayer coverage, while a pronounced decrease in the differential heat of adsorption with increasing oxygen precoverage suggests that the dissociation of molecular oxygen might become an activated process. At about 0.5 ML of oxygen on the (110) surface, the energy gain by adsorbing an additional O atom is comparable to the energy (per atom) required to dissociate an O_2 molecule.

In view of the evident importance of a deeper understanding of the incipient oxidation of Fe surfaces, it is rather surprising that, to the best of our knowledge, so far no *ab initio* investigations of O_2 dissociation on O-precovered Fe surfaces have been performed. The present investigation aims to fill this gap. We present the results of density-functional calculations of the potential-energy profile for O_2 dissociation on clean and partially oxygen-precovered surfaces as a function of increasing coverage and report detailed results for the chemical bonding and for the variation of the electronic and magnetic properties of the impinging oxygen molecules along the reaction path for dissociation.

II. COMPUTATIONAL DETAILS

All calculations have been performed by using density-functional theory as implemented in the Vienna *ab initio* simulation package (VASP).[25] Electronic exchange and correlation effects are treated in a generalized-gradient approximation (GGA) by using the spin-polarized version of the Perdew–Wang[26] (PW91) functional. It is important to emphasize that the GGA is necessary to achieve a correct description of the structural and magnetic ground state of bulk iron.[27,28] The electron–ionic core interactions are treated in the projector-augmented-wave[29] (PAW) formalism. The PAW approach is a genuine all-electron approach and avoids the necessity to include nonlinear corrections to the valence-core interactions. A plane-wave basis with a 400 eV energy cutoff was used. In all calculations, we apply the lattice constant of 2.844 Å, which we previously[30] determined to give the bulk properties of bcc Fe in good agreement with experiment. Our previous studies of the adsorption of atomic oxygen on Fe surfaces were based on ultrasoft pseudopotential calculations. The improved accuracy of the PAW approach leads to adsorption energies larger by about 0.1 eV/atom on Fe(100) and by 0.2–0.5 eV/atom on Fe(110). We note that the larger differences occur only at a coverage for which the O layers are already unstable relative to the formation of a bulk oxide (see below for details).

Both surfaces were modeled by periodically repeated slabs consisting of five Fe layers separated by a vacuum layer of $\simeq$15 Å. A 3×3 surface unit cell allows us to vary the Fe coverage of the surface in increments of 0.11 ML. Brillouin zone integrations were performed by using a $3\times3\times1$ Monkhorst–Pack grid.[31] To accelerate k-point convergence, a Methfessel–Paxton[32] smearing with a width of 0.2 eV was used. The adsorbates were placed on one side of the slab only and a dipole correction[33,34] was applied to compensate for the electrical field gradient through the slab. The positions of Fe atoms in the three topmost layers and the coordinates of all O atoms were optimized until the forces on all unconstrained atoms converged to less than 0.025 eV/Å.

To determine the potential-energy profile for the dissociation of an incoming O_2 molecule, the nudged elastic band (NEB) method[35,36] was used. For each intermediate state along a reaction path connecting the initial and final states, the total energy is minimized in the subspace perpendicular to the reaction coordinate, while the position along the reaction path is kept fixed. The final state for dissociation is determined by the results of our previous studies of the adsorption of atomic oxygen on Fe(100) and Fe(110). On the (100) surface, the stable adsorption site for oxygen is in the fourfold hollows (fh); on the (110) surface, it is the long-bridge (lb) position as determined by *ab initio* calculations,[18,19,37] which are in agreement with experiments.[17,38,39] Hence, the final state for O_2 dissociation are two neighboring lb sites connected via a short-bridge (sb) site on the (110) surface, and two neighboring fh sites connected via a bridge (br) site on the (100) surface. The initial state was an oxygen molecule with the center of gravity located 4 Å above the sb or br sites, respectively, and with the molecular axis pointing via the final adsorption sites. The reaction coordinate is the z coordinate of the center of gravity of the O_2 molecule, and the onset of dissociation is monitored by the stretching of the intramolecular bond length. Note that the NEB method does not restrict lateral displacements or a canting on the incoming molecule that might be induced by interactions with preadsorbed O atoms. The NEB calculations determine the potential-energy profile along the bottom of the reaction channel.

The potential energy of an oxygen molecule approaching the clean or oxygen-precovered iron surface is calculated as the total energy difference with respect to the total energy of the slab representing this surface, E^X, and the energy of an O_2 molecule in the gas phase, E^{O_2}, according to

$$E = \frac{1}{2}(E^{O_2/X} - E^X - E^{O_2}), \tag{1}$$

where $E^{O_2/X}$ stands for the total energy of the system consisting of the iron substrate (eventually, plus predissociated oxygen atoms) and the approaching O_2 molecule (or O atoms, depending on whether the dissociation has already taken place). Hence, the energy difference defined by Eq. (1) measures the differential heat of adsorption of oxygen atom on a

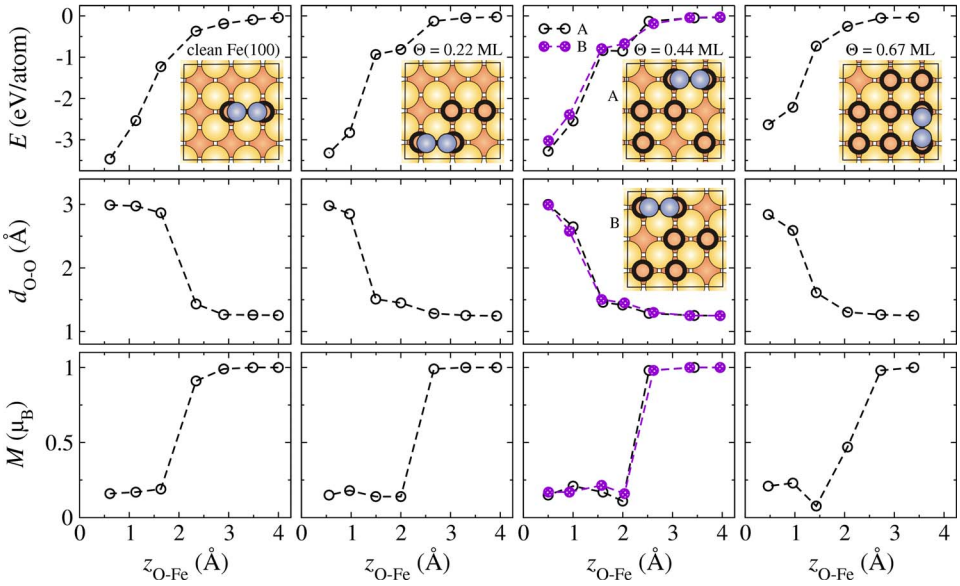

FIG. 1. (Color online) Potential-energy profile and the variation of the calculated O-O bond length, d_{O-O}, and the averaged magnetic moment (per O atom), M, with the oxygen distance to the Fe(100) surface, z_{O-Fe}. Insets display initial, molecular (filled circles), and final atomic configurations (open circles).

precovered surface. The oxygen precoverage Θ is defined as the ratio of the number of adsorbed atoms to the number of atoms in an ideal substrate layer.

If, in addition, at a fixed distance from the surface the variation of the total energy as a function of the O-O distance is monitored, a two-dimensional cut through the potential-energy surface (a so-called elbow plot) is constructed.

The calculated bond length of an O_2 molecule in the gas phase is 1.22 Å and the atomization energy is 143 kcal/mol (note that an increased plane-wave cutoff of 700 eV is required to achieve perfect convergence for the free molecule[40]). The corresponding experimental values are 1.208 Å (bond length) and 118 kcal/mol (atomization energy).[41] It is well known that the large error in the atomization energy of the molecule can be corrected by adopting a hybrid functional.[42] However, it has also been established that all currently known hybrid functionals perform badly for metals (and, in particular, for itinerant magnets).[43,44] Therefore, the only possible choice for the adsorbate/substrate system are the conventional GGA functionals such as those adopted in the present study. We have also checked that for the adsorbate/substrate complex, it is legitimate to choose a lower cutoff energy than for the gas-phase molecule without introducing any significant error in the calculated potential-energy profiles.

III. RESULTS AND DISCUSSION

A. Dissociation on clean and oxygen-precovered Fe(100)

Figure 1 shows the potential-energy profile, the equilibrium bond length, and the magnetic moment of an O_2 molecule approaching the clean or partially precovered Fe(100) surface as a function of the distance of the center of gravity of the molecule from the surface plane. The inset in each panel displays the initial and final positions of the atoms as well as the positions of the preadsorbed oxygen atoms. The local magnetic moments on the oxygen atoms have been calculated by projecting the plane-wave components of all occupied eigenstates onto spherical waves inside an atomic sphere (of the radius r_O=0.82 Å) surrounding the oxygen atoms and integrating the resulting local density of states. Because of the unavoidable overlap of the oxygen spheres with the tails of the eigenstates centered at the Fe atoms of the substrate, the magnetic moments calculated for the dissociated and adsorbed O atoms are never exactly zero, but it is not possible to uniquely separate the physically realistic magnetization induced by the ferromagnetism of the substrate and the magnetism resulting from the overlap of the atomic spheres (which is a mere artifact). Additional information on the differential heat of adsorption (and the final-state geometry), calculated as a function of coverage, is compiled in Table I.

The first column panels in Fig. 1 show that O_2 dissociation on a clean Fe(100) substrate is a nonactivated, strongly exothermic process. On approaching the Fe surface, the stretching is only modest up to a distance of about 2.25 Å, at smaller distances, the O-O distance abruptly increases, which signals dissociation. The strong elongation of the O-O distance between $z \simeq 2$ and 1.7 Å is accompanied by a sudden disappearance of the magnetic moment. Adsorption induces a buckling of the Fe substrate and an incipient outward relaxation of the top layer. For all further details of the final adsorbed configuration, in particular, concerning the magnetism of the substrate, we refer to our earlier work.[18,19]

The configuration for the second dissociation event (O precoverage Θ=0.22 ML) has been chosen such that only one of the additional final adsorption sites is a nearest neighbor to an already preoccupied hollow. This is the largest distance compatible with our 3×3 surface cell. Although dissociation is still nonactivated and the differential adsorption energy shows only a modest decrease (see Table I), significant changes are observed in the reaction scenario: (i) the breaking of the O-O bond occurs only at a much smaller distance ($z \leqslant 1.4$ Å). (ii) The loss of the magnetic moment is observed already at a very modest stretching of the intramolecular bond. (iii) These observations indicate that the modest inflection in the potential energy profile at $z \simeq 2$ Å (not a

TABLE I. The differential adsorption energy E, buckling of the Fe layers, b_i^{Fe}, and of the O adlayer, b^{O}, relaxed interlayer distances in the substrate, d_{ij}, and distance between the oxygen adlayer and the uppermost Fe layer, $z_{\mathrm{O-Fe}}$, calculated for different O coverages, Θ. For labeling of different phases at the 0.67 ML coverage, see insets in Figs. 1 and 3. Note that in Figs. 1 and 3, the O precoverage is given, whereas here Θ refers to the final coverage.

Surface	Θ (ML)	E (eV/atom)	b_1^{Fe} (Å)	b_2^{Fe} (Å)	b_3^{Fe} (Å)	d_{12} (Å)	d_{23} (Å)	b^{O} (Å)	$z_{\mathrm{O-Fe}}$ (Å)
(100)	0.00					1.36	1.45		
	0.22	−3.466	0.08	0.13	0.03	1.42	1.46		0.61
	0.44	−3.320	0.12	0.11	0.01	1.48	1.44	0.02	0.56
	0.67_{A}	−3.277	0.02	0.07		1.54	1.44		0.50
	0.67_{B}	−3.022	0.13	0.10	0.01	1.53	1.44	0.06	0.51
	0.89	−2.635	0.19	0.07	0.01	1.60	1.43	0.02	0.46
(110)	0.00					1.99	2.01		
	0.22	−3.443	0.09	0.03	0.01	2.00	2.01		1.07
	0.44	−2.957	0.25	0.08	0.02	2.01	2.01	0.12	1.11
	0.67_{A}	−2.045	0.25	0.06	0.02	2.03	2.01	0.18	1.12
	0.67_{B}	−1.728	0.37	0.12	0.03	2.05	2.01	0.25	1.14
	0.89	−1.396	0.34	0.13	0.06	2.07	2.02	0.31	1.07

real local minimum) is significant—it indicates the existence of a very short-lived molecular precursor in a nonmagnetic peroxo (O_2^{2-}) state.

A similar scenario applies to O_2 dissociation at a precoverage of $\Theta=0.44$ ML. In this case, we have explored two different configurations, as shown in the inset of Fig. 1. In configuration A, the atoms of the dissociating molecule have each only one O atom in a nearest-neighbor position, while in configuration B, one atom has two O nearest neighbors. Again, we find indications for the existence of a precursor state. The energies of this state are −0.814 and −0.852 eV/atom (−0.672 eV/atom) at heights of 1.999 and 1.998 Å (2.036 Å) above surfaces precovered with 0.22 and 0.44 ML of oxygen, respectively (numbers in parentheses refer to configuration B at 0.44 ML). In this precursor state, the molecule axis is tilted with respect to the surface plane, but the difference in the heights of the O atoms forming the molecule, Δz, does not exceed 0.2 Å. The O-O bond length is stretched to 1.45 and 1.434 Å (1.416 Å), and the magnetic moment decreases to a very low value of $\simeq 0.1\mu_B$. The bond length calculated for this precursor state is almost the same as found by Eichler *et al.* for a peroxo-like precursor on Pt(111).[2] Due to repulsive interactions between the adsorbed oxygen atoms, the final configuration A is lower in energy by 0.255 eV/atom.

To investigate the possible existence of a precursor mechanism more closely, we have calculated the potential energy of the impinging molecule as a function of the O-O bond length along the entire reaction channel, which produces the elbow plot shown in Fig. 2 for the clean and 0.22 ML precovered Fe(100) surfaces. The result for the clean surface is characteristic of direct and barrierless dissociation: the O_2 molecule enters the dissociation channel at a height of 4 Å and with a bond length of 1.22 Å, and its energy decreases monotonously, leading to a minimum at a distance of 0.61 Å from the surface. On the precovered surface, we find a broad plateau of the potential energy at the bottom of the reaction channel extending from $z \approx 1.7$ to 1.35 Å.

Figure 3 shows the difference-electron densities calculated for the precursor state at two different rates of precoverage. The picture demonstrates the electron transfer to antibonding $2\pi^\star$ states of the oxygen molecule, which is accompanied by an only very modest accumulation of electrons in bonding states between adsorbate and substrate. The formation of strong adsorbate-substrate bonds occurs only after the molecule approaches the surface more closely. Our result is in agreement with the observation[7] that at low temperature, the adsorption of O_2 on the Fe(100) surface occurs through a mobile precursor.

The reaction scenario changes at a precoverage of 0.67 ML. A prerequisite for the dissociative adsorption of a fourth O_2 molecule is that two vacant hollow sites in nearest-neighbor positions are available. Only the energetically less favorable final-state configuration B of the preceding adsorption event satisfies this condition; in configuration A, the remaining vacant sites are only next-nearest neighbors. The potential-energy profile shows that dissociation remains a nonactivated process, but the differential heat of adsorption decreases to 2.64 eV/atom, and the profile shows no indication of a precursor state. Bond stretching and demagnetization of the impinging molecule are more continuous processes than in the earlier dissociation steps.

An analysis of the variation of the final-state configurations with increasing oxygen coverage shows two main trends: (i) the adsorbed oxygen atoms sink deeper into the hollows and the buckling of the O layer is very modest. (ii) The adsorbate-induced outward relaxation of the top Fe layer increases with coverage and the Fe layer also shows a quite pronounced buckling. Magnetic moments on the substrate atoms increase with increasing coverage, which reach at full

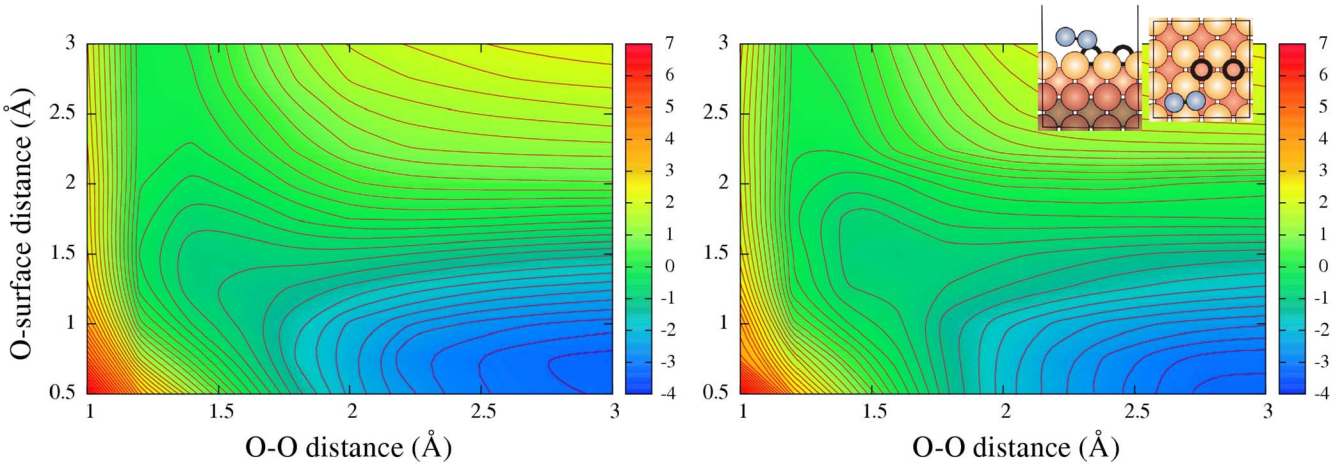

FIG. 2. (Color online) Contour graph for the potential energy of O_2 molecule approaching a clean (left panel) and an O-precovered ($\Theta=0.22$ ML) Fe(100) surface (right panel) as a function of the O-O bond length and the height of the oxygen above the surface. The contour interval is 0.2 eV. The insets display the geometry of the adsorbate/substrate complex at the potential-energy plateau for the impinging molecule at $\approx$1.5 Å to the surface.

monolayer coverage values comparable to the local magnetic moments in the antiferromagnetic Fe oxides. However, the surfaces remain ferromagnetic—we refer to our earlier work for a more detailed discussion.[18,19]

To complete the analysis, we report in Fig. 4 the surface energies as a function of the oxygen chemical potential, as calculated in the grand canonical ensemble.[18,45,46] In agreement with our previous results, we find that the O-covered surfaces are stable with respect to a bulk Fe oxide (the relevant reference is FeO or wustite) up to the highest coverage. However, we also find that the different energies of configurations A and B at $\Theta=0.67$ have a significant influence on the dissociation process. The low-energy configuration A is the stable surface phase over a wide range of chemical potentials, almost up to the limit set by the energy of the bulk oxide. Hence, although dissociation at this coverage is still a nonactivated process, provided that nearest-neighbor surface vacancies exist, the repulsive interactions between adsorbates prevent the formation of such a distribution of adsorbates, which limits the saturation coverage to $\Theta\approx0.67$ ML.

B. Dissociation on clean and oxygen-precovered Fe(110)

The potential-energy profiles for O_2 dissociation on the close packed clean and precovered (110) surfaces are shown in Fig. 5. The information on the geometries and energetics of the final configurations is compiled in Table I. On the clean surface, O_2 dissociation is a nonactivated, strongly exothermic process. At a low coverage of 0.22 ML, the adsorption energies on the (100) and (110) surfaces are almost exactly the same. The equilibrium adsorption sites are the

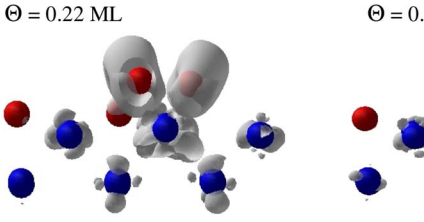

FIG. 3. (Color online) Surfaces of constant electron-density difference (0.007 $e/\text{Å}^3$) for the "precursor" state for O_2 dissociation on an Fe(100) surface precovered with 0.22 and 0.44 ML of O. Only the accumulation of electron charge is displayed.

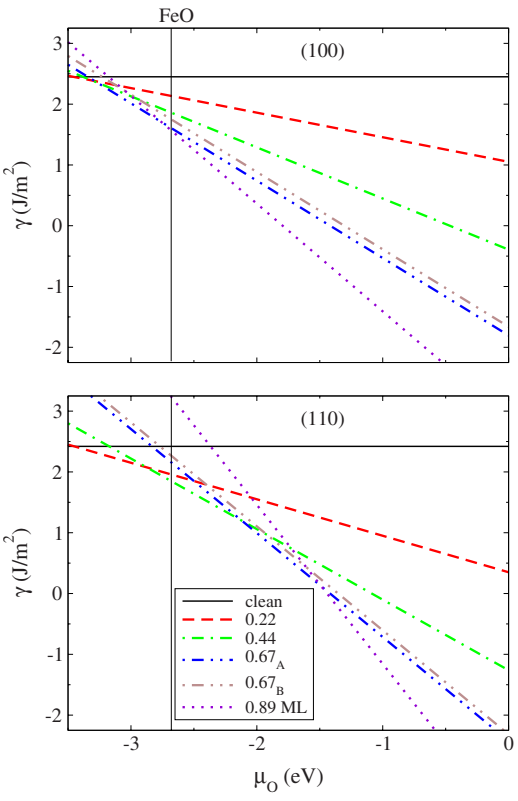

FIG. 4. (Color online) Surface energy of the oxygen-covered Fe (100) and (110) surfaces as a function of the oxygen chemical potential. The vertical lines mark the upper limit to the chemical potential beyond which the formation of a bulk iron oxide (FeO or wustite) is energetically favored.

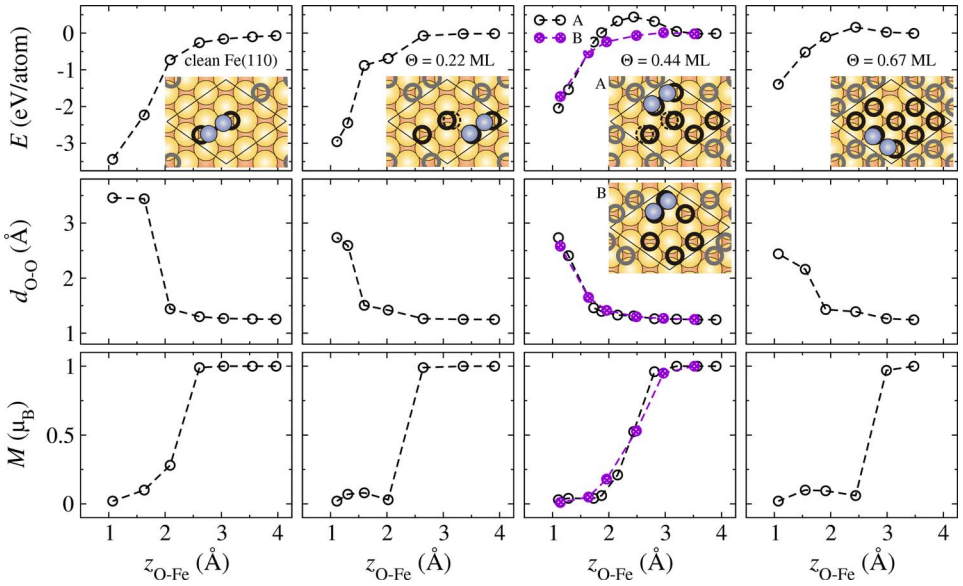

FIG. 5. (Color online) Potential-energy profile and variation of the O-O bond length, d_{O-O}, and of the average magnetic moment of the impinging molecule (per O atom), M, with the distance of the center of gravity of the molecule from the surface, z_{O-Fe}. Insets display the initial molecular (filled circles) and final atomic configurations (open circles). Note that repulsive interactions may induce displacements of preadsorbed oxygen atoms: the atoms depicted by a dashed circle move first during O_2-O/Fe(110) adsorption to the long-bridge position and then relax back into the pseudo-threefold hollow site.

pseudo-threefold hollows (pth). This is in contrast to our previous results based on calculations with a 2×2 surface cell where we found adsorption in lb sites. The different predictions for the equilibrium sites result from the varying impact of repulsive lateral interactions between the adsorbed atoms. In the large 3×3 cell used in the present study, steric repulsions drive the two adsorbed atoms from the neighboring lb to the pth sites, which admit a slightly larger O-O distance. In a 2×2 cell, an isolated O atom is adsorbed in a lb site, and this remains the stable adsorption site also at higher coverage. The occupation of two sites leads to a coverage of 0.5 ML, and the steric interactions between atoms in the periodically repeated cells balance the repulsions between the atoms in the same cell—equilibrium is achieved for atoms in lb sites.

The adsorption of molecular oxygen on a surface precovered with 0.22 ML oxygen follows the same scenario as O_2 dissociation on the precovered Fe(100). The potential-energy profile shows a slight inflection at the energy of −0.692 eV/atom and at a distance from the surface of 2.02 Å (in a tilted position, $\Delta z=0.3$ Å), with an O–O bond length stretched to 1.419 Å. In this state, the molecule has lost its magnetic moment (the projection on the atomic spheres yields $0.03\mu_B$). Hence, prior to dissociation, the molecule goes through a nonmagnetic peroxo-like state, although this is not a true precursor state in the absence of a real potential-energy minimum. However, in contrast to the more open Fe(100) surface, O precoverage of the Fe(110) surface leads to a pronounced decrease of the differential heat of adsorption, which drops by almost 0.5 eV/atom. It is worth noting here that repulsive interactions between the adsorbed O atoms induce a rearrangement in the already adsorbed O adlayer, as schematically depicted in the inset in Fig. 5: one of the oxygen atom adsorbed in a pth site at $\Theta=0.22$ ML moves to a lb position after the second dissociation event. The lateral displacement is also accompanied by a modest change in the magnetic moment: the magnetic moment of the O atom in the lb site is $0.06\mu_B$, while the moment of the oxygen atoms adsorbed in pth sites is almost zero ($0.02\mu_B$/O atom).

At higher oxygen precoverages ($\Theta=0.44$ ML), we have explored two configurations differing in the final locations of the adsorbed O atoms (see the insets in Fig. 5). In configuration A, adsorption takes place in two nonequivalent sites: one with two, the other with only one nearest-neighbor O atom. In this case, adsorption is an activated process, with a barrier of about 0.5 eV/atom. In configuration B, both final adsorption sites have only one O neighbor, and the potential-energy profile shows a monotonous decrease along the entire reaction channel. Thus, at a precoverage of 0.44 ML, the activated and barrierless dissociation channels coexist. The nonactivated reaction also leads to a significantly higher differential adsorption energy. The difference is 0.32 eV/atom and implies that at this precoverage, a steering effect may play a role in the dissociation process.

The transition state identified for configuration A is located at a distance of 2.5 Å from the surface, where the O–O bond length is about 1.3 Å and the molecule retains a magnetic moment of $1\mu_B$ with an orientation antiparallel to the magnetic moment of the substrate atoms. This means that at the transition state, the oxygen molecule assumes a superoxo-like (O_2^{1-}) state and couples antiferromagnetically to the substrate.

Figure 6 shows the difference-electron densities calculated for the precursorlike state at $\Theta=0.22$ ML and for the transition state at $\Theta=0.44$ ML. These graphs visualize the transfer of electrons into the antibonding $2\pi^\star$ state of the dissociating molecule, but—unlike on the Fe(100) surface—also the incipient accumulation of a bond charge representing the adsorbate-substrate bond. The lower part of the figure shows the magnetization density associated with the remaining magnetic moment of the superoxo transition state, which demonstrates the rather localized character of the magnetic moment.

On a surface covered with 0.67 ML of oxygen, further dissociative adsorption of molecular oxygen is possible only starting from the energetically less favorable configuration B because only in this configuration do two vacant nearest-neighbor sites exist. The potential-energy profile shows only

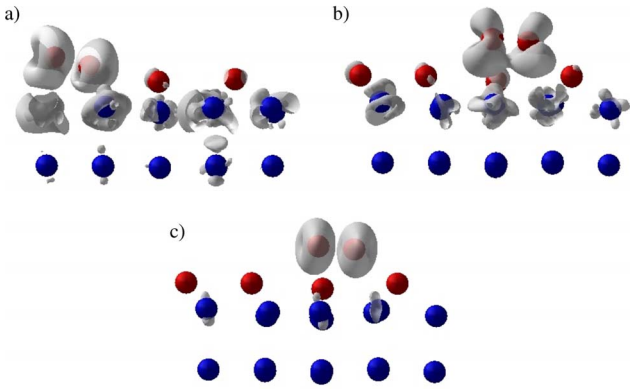

FIG. 6. (Color online) Surface of constant electron density difference (0.007 $e/Å^3$) (a) for the precursorlike state for O_2 dissociation on an Fe(110) surface precovered with 0.22 ML and (b) for the transition state for dissociation at $\Theta=0.44$ ML (configuration A). Only the accumulation of electron charge is displayed. (c) Magnetization density of spin-down electrons corresponding to -0.07 $e/Å^3$ at the transition state.

a minimal reaction barrier of ≈0.1 eV/atom. The intramolecular O–O bond is broken when the molecule approaches the surface at ⩽1.8 Å, but the molecule loses its magnetic moment already at a distance of ≈2.5 Å. The differential heat of adsorption is further reduced to −1.4 eV/atom. In addition, the variation of the surface energy with the chemical potential of oxygen above the surface shows that already at $\Theta \geqslant 0.45$ ML, the O-covered Fe(110) surface becomes unstable against the formation of a bulk oxide layer (see Fig. 4). This is in agreement with our previous results[18] for smaller surface cells.

Hence, the strong decrease in the differential heat of adsorption and in the surface energy with increasing O coverage as well as the appearance of a dissociation barrier indicate that on the close packed Fe(110) surface, saturation is already reached at a coverage of about 0.4 ML. In a strongly oxidizing atmosphere, oxygen atoms will diffuse into the bulk, which contributes to the formation of a bulk oxide. Our findings are supported by experiments by Vescovo *et al.*,[20] according to which a $p(1\times1)$ oxygen overlayer (corresponding to a fully covered surface) is not formed even at 300 K, and by ultraviolet photoemission spectroscopy measurements by Pirug *et al.*,[47] which suggest that oxygen penetrates into the bulk already at $\Theta > 0.4$ ML.

Table I summarizes the results for the differential adsorption energies and the structural characteristics for the final configurations. The differential heat of adsorption decreases very strongly with increasing precoverage. At 0.67 ML of oxygen, it reaches only about 40% of the value calculated for a clean surface. The adsorption geometry also significantly differs from that on the Fe(100) surface: the distance of the O overlayer from the surface is about twice as large and adsorption in pseudo-threefold hollows coexists with adsorption in long-bridge sites, depending on the local adsorbate distributions. The coexistence of different adsorption sites is also reflected in a rather substantial buckling of the O overlayer, which reaches 0.3 Å at the highest coverage. O atoms adsorbed in the lb positions sink deeper into the surface than those adsorbed in pth sites.

IV. SUMMARY AND CONCLUSION

We have presented detailed density-functional theory studies of the dissociative adsorption of molecular oxygen on clean and O-precovered Fe (100) and (110) surfaces. Together with our earlier investigations of the adsorption of atomic oxygen,[18,19] the additional results provide a rather complete picture of the incipient oxidation of iron surfaces. The adsorption of atomic oxygen is a direct and barrierless process on both clean surfaces. A partial precoverage with oxygen only leads to a linear decrease of the differential heat of adsorption on (110), while on (100), adsorption is almost unaffected by preadsorbed oxygen. In contrast, the scenarios for the dissociative adsorption of molecular oxygen are distinctly different.

On Fe(100), a nonactivated reaction channel may be found even on a surface nearly completely covered with oxygen. However, as dissociation requires at least two vacant sites in neighboring hollows, the probability that an impinging molecule enters such a barrierless channel, which leads to dissociation, decreases with increasing oxygen coverage. This observation explains that at low temperatures, the sticking probability remains close to unity up to $\Theta \approx 0.8$ ML, while at room temperature, it begins to decrease already for $\Theta \geqslant 0.35$ ML: it is well known that steering effects guiding the molecule toward the most favorable reaction channels are more efficient at low temperatures and low kinetic energies. For low and intermediate O precoverages ($\Theta=0.22$ and 0.44 ML), our calculated potential-energy profiles display a plateau (or even a very shallow minimum) at a distance of about 1.5 Å above the surface. The O–O bond length and the magnetic moment of the O_2 molecule correspond to a peroxo-like (O_2^{2-}) precursor state. The existence of a highly mobile precursor had been postulated on the basis of the coverage dependence of the sticking probability measured at low temperatures.

On the Fe(110) surface, we find activated and nonactivated channels for O_2 dissociation already at $\Theta=0.44$ ML, which depend on the distribution of the preadsorbed O atoms. The transition state corresponds to a magnetic superoxo-like (O_2^{1-}) configuration. It is important to emphasize that the activated reaction channel leads to an energetically more favorable distribution of the O atoms, but one that hinders further dissociative adsorption. These results agree with the observation that upon exposure to molecular oxygen, saturation occurs already at $\Theta \sim 0.4$, while the adsorption of atomic oxygen leads to the formation of ordered oxide films, which is in agreement with our earlier results. That the formation of an oxide films is favored over the formation of a denser O overlayer also agrees with our results on the variation of the surface energies with the chemical potential of oxygen in the reactive atmosphere.

ACKNOWLEDGMENTS

The Wien-Wrocław cooperation has been initiated by the Marie-Curie Training Site "Atomic-scale computational materials science" at the Universität Wien. Work in Wrocław was partly supported by the Polish Ministry of Science within the Research Project No. 1 P03B 114 28.

*Corresponding author: piotr.blonski@univie.ac.at
†kiejna@ifd.uni.wroc.pl
‡juergen.hafner@univie.ac.at

[1] A. Eichler and J. Hafner, Phys. Rev. Lett. **79**, 4481 (1997).
[2] A. Eichler, F. Mittendorfer, and J. Hafner, Phys. Rev. B **62**, 4744 (2000).
[3] B. C. Stipe, M. A. Rezaei, W. Ho, S. Gao, M. Persson, and B. I. Lundqvist, Phys. Rev. Lett. **78**, 4410 (1997).
[4] M. Alatalo, A. Puisto, H. Pitkänen, A. S. Foster, and K. Laasonen, Surf. Sci. **600**, 1574 (2006).
[5] A. Gross, B. Hammer, M. Scheffler, and W. Brenig, Phys. Rev. Lett. **73**, 3121 (1994).
[6] A. Eichler, J. Hafner, A. Gross, and M. Scheffler, Phys. Rev. B **59**, 13297 (1999).
[7] J. P. Lu, M. R. Albert, S. L. Bernasek, and D. J. Dwyer, Surf. Sci. **215**, 348 (1989).
[8] A. M. Horgan and D. A. King, Surf. Sci. **23**, 259 (1970).
[9] C. R. Brundle, Surf. Sci. **66**, 581 (1977).
[10] C. R. Brundle, IBM J. Res. Dev. **22**, 235 (1978).
[11] H. Viefhaus and H. J. Grabke, Surf. Sci. **109**, 1 (1981).
[12] C. Jansson and P. Morgen, Surf. Sci. **223**, 84 (1990).
[13] B. L. Maschhoff and N. R. Armstrong, Langmuir **7**, 693 (1991).
[14] T. Miyano, Y. Sakisaka, T. Komeda, and M. Onchi, Surf. Sci. **169**, 197 (1986).
[15] Y. Sakisaka, T. Komeda, T. Miyano, M. Onchi, S. Masuda, Y. Harada, K. Yagi, and H. Kato, Surf. Sci. **164**, 220 (1985).
[16] V. S. Smentkowski and J. T. Yates, Surf. Sci. **232**, 113 (1990).
[17] A. Wight, N. G. Condon, F. M. Leibsle, G. Worthy, and A. Hodgson, Surf. Sci. **331-333**, 133 (1995).
[18] P. Błoński, A. Kiejna, and J. Hafner, Surf. Sci. **590**, 88 (2005).
[19] P. Błoński, A. Kiejna, and J. Hafner, J. Phys.: Condens. Matter **19**, 096011 (2007).
[20] E. Vescovo, C. Carbone, W. Eberhardt, O. Rader, T. Kachel, and W. Gudat, Phys. Rev. B **48**, 285 (1993).
[21] H. J. Kim, J. H. Park, and E. Vescovo, Phys. Rev. B **61**, 15284 (2000).
[22] K. Koike and T. Furukawa, Phys. Rev. Lett. **77**, 3921 (1996).
[23] K. Mori, M. Yamazaki, T. Hiraki, H. Matsuyama, and K. Koike, Phys. Rev. B **72**, 014418 (2005).
[24] M. Busch, M. Gruyters, and H. Winter, Surf. Sci. **600**, 2778 (2006).
[25] G. Kresse and J. Hafner, Phys. Rev. B **47**, 558 (1993); **49**, 14251 (1994).
[26] J. P. Perdew, J. A. Chevary, S. H. Vosko, K. A. Jackson, M. R. Pederson, D. J. Singh, and C. Fiolhais, Phys. Rev. B **46**, 6671 (1992).
[27] P. Bagno, O. Jepsen, and O. Gunnarsson, Phys. Rev. B **40**, 1997 (1989).
[28] E. G. Moroni, G. Kresse, J. Hafner, and J. Furthmüller, Phys. Rev. B **56**, 15629 (1997).
[29] G. Kresse and D. Joubert, Phys. Rev. B **59**, 1758 (1999).
[30] P. Błoński and A. Kiejna, Surf. Sci. **601**, 123 (2007).
[31] H. J. Monkhorst and J. D. Pack, Phys. Rev. B **13**, 5188 (1976).
[32] M. Methfessel and A. T. Paxton, Phys. Rev. B **40**, 3616 (1989).
[33] J. Neugebauer and M. Scheffler, Phys. Rev. B **46**, 16067 (1992).
[34] L. Bengtsson, Phys. Rev. B **59**, 12301 (1999).
[35] G. Mills, H. Jonsson, and G. K. Schenter, Surf. Sci. **324**, 305 (1995).
[36] H. Jonsson, G. Mills, and K. W. Jacobsen, in *Classical and Quantum Dynamics in Condensed Phase Simulations*, edited by B. J. Berne, G. Ciccotti, and D. F. Coker (World Scientific, Singapore, 1998).
[37] M. Eder, K. Terakura, and J. Hafner, Phys. Rev. B **64**, 115426 (2001).
[38] K. O. Legg, F. P. Jona, D. W. Jepsen, and P. M. Marcus, J. Phys. C **8**, L492 (1975).
[39] C. Leygraf and S. Ekelund, Surf. Sci. **40**, 609 (1973).
[40] A. Kiejna, G. Kresse, J. Rogal, A. De Sarkar, K. Reuter, and M. Scheffler, Phys. Rev. B **73**, 035404 (2006).
[41] K. P. Huber and G. Herzberg, *Constants of Diatomic Molecules*, NIST Chemistry WebBook, NIST Standard Reference Database Number 69 (http://webbook.nist.gov).
[42] J. Paier, R. Hirschl, M. Marsman, and G. Kresse, J. Chem. Phys. **122**, 234102 (2005).
[43] J. Paier, M. Marsman, K. Hummer, G. Kresse, I. C. Gerber, and J. G. Ángyán, J. Chem. Phys. **124**, 154709 (2006).
[44] J. Paier, M. Marsman, and G. Kresse, J. Chem. Phys. **127**, 024103 (2007).
[45] K. Reuter and M. Scheffler, Phys. Rev. B **65**, 035406 (2001).
[46] A. Rohrbach, J. Hafner, and G. Kresse, Phys. Rev. B **70**, 125426 (2004).
[47] G. Pirug, G. Broden, and H. P. Bonzel, Surf. Sci. **94**, 323 (1980).